IOP Conf. Series: Journal of Physics: Conf. Series **874** (2017) 012071 doi:10.1088/1742-6596/874/1/012071

Beam shaping with 4n-order multipole magnets

B Folsom[1,2], **E Laface**[1,2]

[1]Lund University, Particle Physics Division, Lund, Sweden
[2]European Spallation Source ERIC, Lund, Sweden

E-mail: ben.folsom@esss.se

Abstract. A uniformly irradiating beam is beneficial in spallation for preventing irregular wear on the target. For octupoles (n = 4) and higher-order (n = 4N) magnets, passing charged-particle bunches undergo symmetric shaping effects along the x and y axes. Using a Lie-mapping formalism, we illustrate how well Gaussian distributions can be flattened symmetrically in 2D with single, dual-pulse, and RF magnets of 4N order. Incidental shaping effects are also discussed.

1. Introduction

For charged particle or ion bunches, an octupole displaces the outermost particles, reshaping a Gaussian transverse profile to a flattened or concave one [1]. Inherent to this flattening property is a four-fold rotational symmetry octupoles impart on transverse beam distributions (specifically, symmetry along each x–y diagonal).

Because of this, it is standard practice to introduce octupoles in pairs with respective quadrupoles so that their effects are only appreciable along one axis. This negates the defocusing of off-center particles near the diagonals. Such an approach is common when correcting high-order errors in beam-focusing or beam-steering optics [1–4].

With this single-axis flattening, however, a number of transverse and longitudinal shaping phenomena are disregarded. This study considers such effects, beginning with a discussion of the octupole and octupole-like Hamiltonians in a symplectic Lie-algebra formalism. It is shown that x–y decoupled, alternating-gradient, and dual-pulse multipoles can act on transversely symmetric 2D bunches to induce a variety of shaping effects such as low-loss flattening, isotropic focusing, transverse trapping, and longitudinal momentum dilation.

2. 4N-Pole Symmetry

In previous works, we reviewed the Lie-algebra formalism which implicitly preserves symplecticity in calculating the trajectories of bunched particles under nonlinear potentials [5,6]. In this approach, a position or momentum coordinate can be tracked as

$$c = e^{-t:H:}c_0 \ , \tag{1}$$

where t is traversal time through the element, H is the machine-element's Hamiltonian, and the colons denote Lie brackets: $\left(\frac{\partial f(x,p)}{\partial x}\frac{\partial g(x,p)}{\partial p} - \frac{\partial g(x,p)}{\partial x}\frac{\partial f(x,p)}{\partial p}\right)$. These absorb any variable falling to the right as the $g(x,p)$ term. Here, the exponential can be expanded in series and truncated

IOP Conf. Series: Journal of Physics: Conf. Series **874** (2017) 012071 doi:10.1088/1742-6596/874/1/012071

at a desired precision (resulting in nested Lie brackets) or simplified with Yoshida's symplectic integration approach [7].

The component of the Hamiltonian corresponding to the external potential from a multipole magnet can be represented as a complex binomial:

$$K(x+iy)^n \ , \tag{2}$$

where the real and imaginary terms correspond to normal and skew orientations, respectively. To derive the field gradient K, we begin with [8, 9]:

$$\kappa_n = \frac{e \cdot B_0}{\vec{p}_{\|}(n-1)!\ a_0^{(n-1)}}[\mathrm{m}^{-n}] \ , \tag{3}$$

where e is particle charge, $\vec{p}_{\|}$ is longitudinal momentum, and B_0 and a_0 are the pole-tip magnetic flux and radius, respectively. Noting that any binomial expansion results in terms of cumulative order n, the potential term for a normal multipole

$$\kappa_n \cdot \mathfrak{Re}(x+iy)^n \ , \tag{4}$$

is thus unitless. We can then normalize to

$$K_n = \kappa_n \cdot \mathrm{K_E} \ , \tag{5}$$

where $\mathrm{K_E}$ is kinetic energy. This results in a Hamiltonian with units of energy:

$$H_n = K_n \cdot \mathfrak{Re}(x+iy)^n + \frac{\vec{p}_{\perp}^{\,2}}{2m} \ . \tag{6}$$

Lie-algebra tracking with this normalization has been cross-checked with the beam-physics simulation package Tracewin [10] for the results to follow, unless otherwise noted.

For a normal octupole, the potential term is

$$K_4(x^4 - 6x^2y^2 + y^4) \ , \tag{7}$$

What is noteworthy here is that the leading-order terms are both positive (since $\mathrm{i}^{4n} = 1$), resulting in the observed four-fold rotational symmetry. This carries for higher-order 4n-pole magnets, where the sign parity of like-order terms ensures identical distributions along the x and y axes. For example, the potential term for the hexadecapole is

$$K_8(x^8 - 28x^6y^2 + 70x^4y^4 - 28x^2y^6 + y^8) \ . \tag{8}$$

To generalize, any $n = 4\mathrm{N}$ pole magnet could be considered "octupole like", with all other $n = 2\mathrm{N}$ pole magnets as "quadrupole like". In the latter case, x and y profiles may have symmetry about their own axes, but their profile shapes are always dissimilar. For both cases, as the number of poles is increased, the shaping effect converges toward a circular 2D profile, with particles along the circumference forming narrowing cusps.

3. Decoupling

Recent works have demonstrated that octupoles can be virtually decoupled in a periodic lattice by using quadrupole and dipole inserts on either side of an octupole [11, 12]. That is,

$$H_4 = K_4(x^4 - \cancel{6x^2y^2} + y^4) \ . \tag{9}$$

Figure 1 illustrates that such a magnet may be used for improved beam flattening. Since decoupled multipoles are not implemented into Tracewin, these simulations were carried out solely with an ab-initio Lie-algebra code, using rudimentary space-charge kicks on either side of the magnet:

$$p = p_0 + \frac{C}{2}\,\mathrm{erf}\left(\frac{x}{\sigma_x}\right) \ , \tag{10}$$

with

$$C = \frac{It}{6\pi} \ , \tag{11}$$

where I is beam current and the factor of $1/2$ in equation (10) reflects a halving of the magnet length and "erf" is the error function. This equation was verified to match Tracewin for Gaussian distributions in drift spaces with wide enough apertures to avoid image effects.

A key trait of the decoupled octupole is its virtually lossless flattening: a coupled magnet of matched strength can only produce a similarly flattened profile by ejecting a significant percentage of its outermost particles. For example, the coupled octupole in figure 1a loses 1% of its particles to beyond $6\,\sigma_x$ whereas the decoupled octupole's losses are 0.1%.

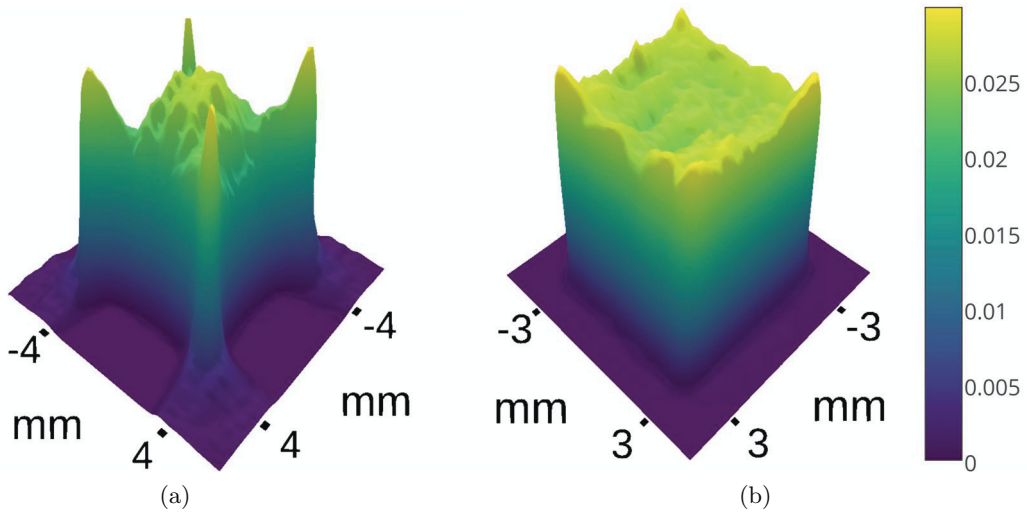

Figure 1. Surface plot of Gaussian distributions (100k protons) passing through (a) coupled and (b) uncoupled octupoles, normalized to maximum bin occupancy. Beam and magnet parameters are otherwise identical: $a_0 = 25$ [mm], $\epsilon_\perp = 0.5$ [$\pi \cdot$ mm $\cdot$ mrad], $\beta_\perp = 1$ [mm/($\pi \cdot$ mrad)], $B_0 = 3$ T, $K_E = 4$ MeV, I = 30 mA, and magnet length $L = 500$ mm.

As field strength is increased, focusing can also be observed in decoupled magnets with a reduced loss rate (i.e. a reduction of σ_x by 50% with ∼7% ejecta for decoupled magnets and $\gtrsim$30% for coupled magnets).

However, the use of equation (9) in obtaining these results must be considered an idealization, since in practice, the inserts required for virtual decoupling are calibrated via thin-lens approximation.

4. RF Octupoles

Although better flattening can be achieved with coupled octupoles than that of figure 1a, it typically requires a significant dilation of the transverse dimensions. This can be improved if

we consider alternating-current $n = 4N$ pole magnets operating between 1 MHz and 1 THz. For the present work, this effect was simulated with stepped waves (i.e. successive kicks of $-9, -6, -3, 0, 3, 6, 9$ T as one half-cycle).

For low field strength–emittance ratios, this effectively creates a virtual aperture: Initially, a shell of the outermost particles is lost in the first few cycles. After a few hundred cycles (~ 100 mm), the beam distribution tends toward a conical shape and with a reduced loss rate. This effect holds for Gaussian distributions, but is more easily observed with waterbag or KV distributions. When accounting for space charge, the shaping effects are similar, with losses occurring at a constant rate proportional to beam current. At higher field strengths, losses can be eliminated altogether, with transverse positions effectively trapped after an initial dilation.

Figure 2 shows the longitudinal effects of trapping a 50 MeV electron beam. With an initial $\sigma_{z'}$ of 0.0005 mrad, the longitudinal momentum quickly dilates symmetrically (figure 2a). Particles with high transverse momenta then begin to recirculate in the positive z' direction (figure 2b). Here, an extremely small pole-tip aperture is used to exaggerate the effect — with more realistic parameters, a dilation in momentum of a factor of 10 can be observed, with a similar concentration of the electron population in the positive z' direction.

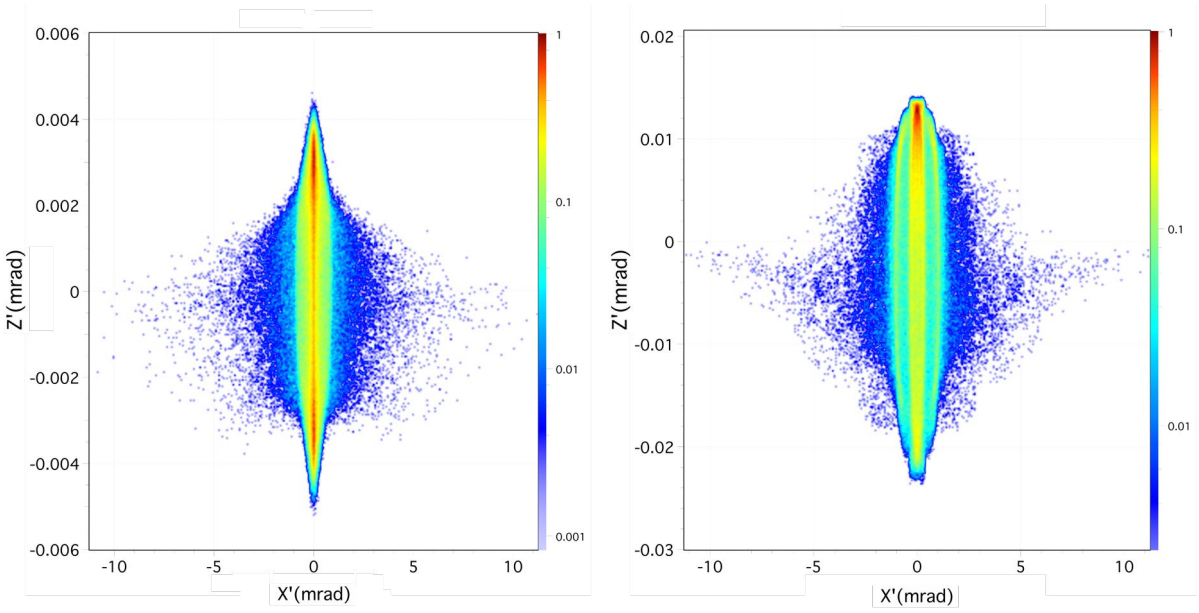

(a) (b)

Figure 2. Transverse–Longitudinal density mapping for 500k electrons in a 30 GHz RF octupole at (a) 40 mm and (b) 400 mm; $a_0 = 1$ [mm], $\epsilon_\perp = 0.25$ [$\pi \cdot$ mm $\cdot$ mrad], $\epsilon_\parallel = 0.35$ [$\pi \cdot$ mm $\cdot$ mrad], $\beta_\perp = 4$ [mm/($\pi \cdot$ mrad)], $\beta_\parallel = 5$ [mm/($\pi \cdot$ mrad)], $B_0 = 10$ T, $K_E = 25$ MeV, I = 50 mA.

The cost of such a shift is incurred as emittance gains (proportional to beam current). Here, the longitudinal emittance increases steadily, but transverse emittance levels off quickly as the particles become trapped.

At higher frequencies, hollowing can be observed (figure 3a), with the bunch collapsing centrally as the magnet length is increased (figure 3b). Similar effects were reported in [13–15].

In this case, hollowing can be seen as an extension of beam flattening—a beam becomes approximately flat before its central population is forced toward the halo.

Moreover, at these frequencies but increased field strengths, focusing can be achieved with zero ejecta (which forgoes hollowing and rapidly condenses the central region).

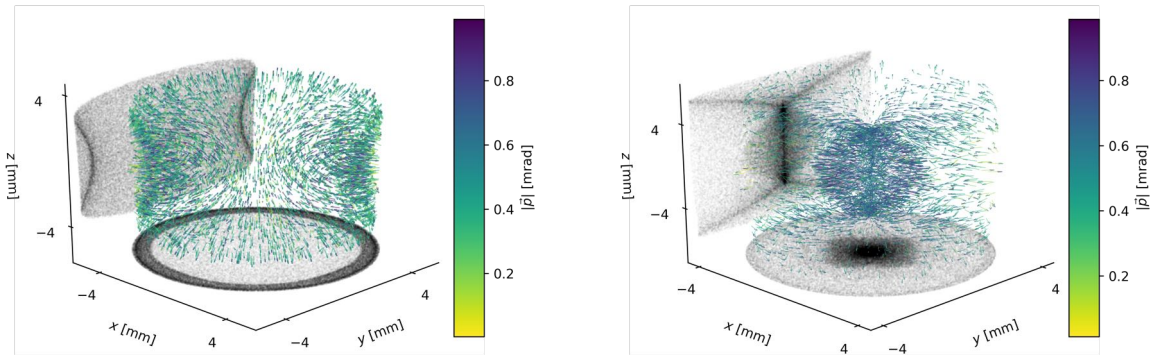

(a) (b)

Figure 3. Beam hollowing and subsequent collapse of electrons (100k, Gaussian) in a 1 THz, $B_{max} = 9$ T, RF octupole: $a_0 = 20$ [mm], $\epsilon_\perp = 0.25$ [$\pi \cdot$ mm $\cdot$ mrad], $\beta_\perp = 4$ [mm/($\pi \cdot$ mrad)], $K_E = 0.75$ MeV, I = 62 mA. Magnets lengths are 0.375 and 0.778 m and momenta are scaled to maxima of 20.9 and 24.5 mrad for (a) and (b) respectively.

5. Double-Pulse Shaping

The aforementioned traits of alternating-gradient multipoles may be worth investigating further, but the fabrication of such devices is likely to require prohibitive stress tolerances or materials costs.

For a more practical design, an initial octupole can provide a brief high-strength pulse so that a passing bunch arrives at the second octupole with a compacted momentum distribution but before its position distribution has been significantly altered. The second magnet then gives a longer, weaker pulse which effectively traps the perturbed central trajectories. This results in a sharper beam flattening than can be achieved with individual magnets, with an improvement comparable to that shown in figure 1. This scheme induces negligible losses when shaping to a bunch perimeter of $\sim 3\sigma_x$. By increasing the initial pulse strength, a width reduction to $\sim 2\sigma_x$ can be achieved with $\sim 1\%$ losses.

6. Conclusions

Octupole and octupole-like magnets are shown to act with four-fold rotational symmetry in the transverse plane. While the effect of such magnets is a flattening of the transverse momentum and position distributions in turn, any rapid, pronounced shaping carries inherent particle losses. To address this, decoupling, high-frequency alternating gradients, and dual-pulse kicks may be beneficial. The incidental phenomena of transverse-beam trapping, longitudinal momentum dilation, and beam hollowing may also merit further study.

References

[1] Tsoupas N, Zucker M S, Ward T E and C L Snead J 1997 *Nuclear Science and Engineering* **126** 71–79 URL http://epubs.ans.org/?a=24458
[2] Meigo S i, Ooi M, Ikezaki K, Akutsu A and Fujimori H 2014 *Proc. IPAC2014, Dresden, Germany* 15–20
[3] Ho D D M, Haber I, Crandall K R and Brandon S T 1991 *Part. Accel.* **36** 141–160 URL http://cds.cern.ch/record/1054399
[4] Brinkmann R and Raimondi P 2001 *Proc. PAC 2001. Chicago, IL, USA* **5** 3828–3830
[5] Laface E 2015 *Proc. IPAC2015, Richmond, VA, USA* 345–347

[6] Folsom B and Laface E 2016 *Proc. IPAC2016, Busan, Korea* 3080–3082
[7] Yoshida H 1990 *Physics Letters A* **150** 262–268 ISSN 0375-9601 URL http://www.sciencedirect.com/science/article/pii/0375960190900923
[8] Wiedemann H 2015 *Particle accelerator physics* (Springer)
[9] Wille K 2000 *The physics of particle accelerators: an introduction* (Clarendon Press)
[10] Uriot D and Pichoff N 2011 *CEA internap report CEA/DSM/DAPNIA/SEA/2000/45*
[11] Antipov S A, Nagaitsev S and Valishev A 2016 *arXiv preprint arXiv:1604.08565*
[12] Nagaitsev S, Valishev A and Danilov V 2012 *arXiv preprint arXiv:1207.5529*
[13] Neuner U *et al.* 2000 *Physical Review Letters* **85** 4518–4521 URL https://link.aps.org/doi/10.1103/PhysRevLett.85.4518
[14] Stancari G, Valishev A, Annala G, Kuznetsov G, Shiltsev V, Still D A and Vorobiev L G 2011 *Physical Review Letters* **107** 084802 URL https://link.aps.org/doi/10.1103/PhysRevLett.107.084802
[15] Blaugrund A E and Cooperstein G 1975 *Physical Review Letters* **34** 461–464 URL https://link.aps.org/doi/10.1103/PhysRevLett.34.461